



Naturalistic Stimuli Increase the Rate and Efficiency of Information Transmission by Primary Auditory Afferents

F. Rieke; D. A. Bodnar; W. Bialek

Proceedings: Biological Sciences, Volume 262, Issue 1365 (Dec. 22, 1995), 259-265.

Stable URL:

<http://links.jstor.org/sici?sici=0962-8452%2819951222%29262%3A1365%3C259%3ANSITRA%3E2.0.CO%3B2-F>

Your use of the JSTOR archive indicates your acceptance of JSTOR's Terms and Conditions of Use, available at <http://www.jstor.org/about/terms.html>. JSTOR's Terms and Conditions of Use provides, in part, that unless you have obtained prior permission, you may not download an entire issue of a journal or multiple copies of articles, and you may use content in the JSTOR archive only for your personal, non-commercial use.

Each copy of any part of a JSTOR transmission must contain the same copyright notice that appears on the screen or printed page of such transmission.

Proceedings: Biological Sciences is published by The Royal Society. Please contact the publisher for further permissions regarding the use of this work. Publisher contact information may be obtained at <http://www.jstor.org/journals/rsl.html>.

Proceedings: Biological Sciences
©1995 The Royal Society

JSTOR and the JSTOR logo are trademarks of JSTOR, and are Registered in the U.S. Patent and Trademark Office. For more information on JSTOR contact jstor-info@umich.edu.

©2003 JSTOR

Naturalistic stimuli increase the rate and efficiency of information transmission by primary auditory afferents

F. RIEKE,^{1,3*} D. A. BODNAR,² AND W. BIALEK¹

¹ *NEC Research Institute, 4 Independence Way, Princeton, New Jersey 08540, U.S.A.*

² *Section of Neurobiology and Behavior, Cornell University, Ithaca, New York 14853, U.S.A.*

³ *Department of Neurobiology, Stanford University, Palo Alto, California 94305, U.S.A.*

SUMMARY

Natural sounds, especially communication sounds, have highly structured amplitude and phase spectra. We have quantified how structure in the amplitude spectrum of natural sounds affects coding in primary auditory afferents. Auditory afferents encode stimuli with naturalistic amplitude spectra dramatically better than broad-band stimuli (approximating white noise); the rate at which the spike train carries information about the stimulus is 2–6 times higher for naturalistic sounds. Furthermore, the information rates can reach 90% of the fundamental limit to information transmission set by the statistics of the spike response. These results indicate that the coding strategy of the auditory nerve is matched to the structure of natural sounds; this ‘tuning’ allows afferent spike trains to provide higher processing centres with a more complete description of the sensory world.

1. INTRODUCTION

The world around us is, thankfully, a highly structured place. This structure is reflected in the fact that the signals which reach our sense organs are not completely random, but rather exhibit correlations both in space and in time. What does the nervous system do with this structure? One possibility, first raised by Barlow (1961), is that even at the sensory periphery the statistical structure of natural signals is important in creating efficient representations of the sensory world. This type of specialization is likely to occur in the initial coding of continuous sensory inputs into discrete action potentials. Do primary sensory afferent spike trains transmit more information when the input stimuli are chosen from natural ensembles? In this paper we address this question directly by comparing the information transmission and coding efficiency for single auditory afferents responding with stimuli chosen from different ensembles.

Testing the hypothesis that primary afferents are ‘tuned’ to natural stimuli requires that we understand the structure of these stimuli. This is a difficult problem. In the olfactory system signals are carried by turbulent air flow, and understanding the statistics and dynamics of these turbulent plumes is still an important physics problem (Shraiman & Siggia 1994). In vision, measurements of the statistics of natural images reveal a hierarchy of structures on all angular scales (Ruderman & Bialek 1994). In the auditory system, stimuli are characterized by their amplitude and phase spectra, and communication sounds with clear behavioural significance have been characterized for many species. So the coding of acoustic communication signals

provides an excellent opportunity to test Barlow’s hypothesis.

We have chosen to study the bullfrog auditory system, which spends much of its time processing rather stereotyped sounds: frog calls. The peripheral auditory system of the bullfrog is a classic system for the investigation of behaviourally relevant stimuli (Frishkopf *et al.* 1968; Capranica & Moffat 1975). Frogs and toads use species-specific communication signals called advertisement calls in their reproductive behaviour (Bogert 1960). These signals have highly structured temporal waveforms. Out of all the possible structure in frog calls we focus on the amplitude spectrum, which consists of several nearly harmonic bands.

Shaping the amplitude spectrum into bands endows stimuli with a finite correlation time, which measures how far into the future the waveform can be predicted given knowledge of the past. The extreme cases are white noise, with a correlation time of zero, and pure tones, with an infinite correlation time. Whereas animals use the temporal correlations of natural stimuli in making behavioural decisions, it is not clear how temporal correlations influence strategies for processing these signals, or at what processing stage structure in the input signals is important. Here we investigate whether the coding mechanisms of primary auditory afferent fibres are matched to the temporal correlations of natural sounds. Specifically, we compare the ability of primary auditory afferent fibres to code broad-band noise and noise shaped to have a naturalistic amplitude spectrum.

We characterize the coding of continuous sensory stimuli in afferent spike trains using two quantitative measures: information rate and coding efficiency

(Bialek *et al.* 1993; Rieke *et al.* 1993). The information rate measures, in bits per second, the rate at which the spike train removes uncertainty about the sensory stimulus. The coding efficiency compares this gain of information or reduction of uncertainty to the physical limits imposed by the statistics of the spike train itself. We shall see that for naturalistic stimuli, but not for white noise, auditory nerve fibres come remarkably close to these physical limits to information transmission.

2. METHODS

(a) *Experimental stimuli*

The amplitude spectrum of a bullfrog advertisement call is composed of approximately 20 harmonically related bands with a fundamental frequency near 100 Hz (Capranica 1968). The width of each of the low-frequency bands is about 30 Hz, corresponding to a correlation time of 100 ms. Our experimental stimuli are broad-band Gaussian noise and Gaussian noise filtered to produce an amplitude spectrum identical to that of a bullfrog advertisement call (the call-spectrum stimulus). Stimuli were generated digitally with a sampling frequency of 8 kHz and stored on a digital-audio tape for presentation during an experiment. We generated the broad-band stimulus by drawing a random number from a Gaussian distribution at every time point. We generated the call-spectrum stimulus in two steps. First, we created broad-band Gaussian noise as above. We then adjusted the amplitude of each frequency component of the stimulus using the amplitude spectrum of a recorded bullfrog advertisement call as a template. The result is a signal with a highly structured amplitude spectrum, but one in which each frequency component is independent.

(b) *Neurophysiological recordings*

The bullfrog has two peripheral auditory organs: the amphibian papilla and the basilar papilla (Capranica 1976). We limited our investigation to the low-frequency fibres of the amphibian papilla (best excitatory frequency (BEF) < 600 Hz), which have coding mechanisms similar to those of auditory fibres in other vertebrates e.g. phase locking (Narins & Hillery 1983; Freedman *et al.* 1988) two-tone suppression (Liff & Goldstein 1970; Shofner & Feng 1981), and difference tone nonlinearities (Capranica & Moffat 1980). Surgery, anaesthesia, and physiological recording protocols and procedures were the same as those described by Bodnar & Capranica (1994). Briefly, we used a ventral approach to expose the VIIIth nerve. A glass micropipette (resistance 40–70 MW, filled with 3 M KCl) recorded from an individual auditory nerve afferent while stimuli were presented via an earphone in a T-tube coupler. One end of the coupler was sealed around the tympanum of the frog; the other end contained a 1.3 cm diameter microphone for measuring the sound pressure waveform. Each stimulus was presented for 5–10 min, during which time the cell generated about 10000 spikes. The first 80–90% of the experiment was used to calculate the estimation filters described below; the remainder of the experiment was used to test the quality of the estimates. In most experiments the intensity level of the stimulus was adjusted such that the average firing rate of a fibre was similar for both broad-band and call-spectrum stimuli, usually 70 dB sound pressure level for the call-spectrum stimulus and 80 dB sound pressure level, 45 dB spectrum level, for the broad-band stimulus. The stimulus waveform measured in the acoustic coupler and the cor-

responding spike response were recorded on separate channels of a digital-audio tape for offline analysis.

(c) *Stimulus estimation, information rate and efficiency*

To measure the rate at which the spike train provides information about the stimulus we decode the measured spike train to estimate the continuous stimulus waveform. This approach has been used in several sensory systems (Bialek *et al.* 1991; Warland *et al.* 1991; Rieke *et al.* 1991). In all the systems studied, the stimulus waveform could be estimated from the spikes by filtering the spike train with a linear filter. Thus our estimate takes the form

$$s_{\text{est}}(t) = \sum_i F(t-t_i), \quad (1)$$

where the spikes occur at times t_i . The estimation filter $F(t)$ is determined by minimizing the mean-square error between the estimate and stimulus $s(t)$,

$$\chi^2 = \langle \int dt |s(t) - s_{\text{est}}(t)|^2 \rangle, \quad (2)$$

i.e. by requiring that $\delta\chi^2/\delta F(t) = 0$; the average $\langle \dots \rangle$ is over the stimulus ensemble. In practice we estimate the ensemble average by averaging over a set of experimental stimuli drawn randomly from the ensemble. The minimization problem can be solved analytically (see Bialek *et al.* 1991), resulting in the frequency-domain filter

$$\begin{aligned} \tilde{F}(\omega) &= \int dt \exp(i\omega t) F(t) \\ &= \frac{\langle \sum_i \exp(i\omega t_i) \tilde{s}^*(\omega) \rangle}{\langle |\sum_i \exp(i\omega t_i)|^2 \rangle}, \end{aligned} \quad (3)$$

where t_i are the spike times, $\tilde{s}(\omega)$ is the Fourier transform of the stimulus $s(t)$, and $*$ denotes the complex conjugate. The filter is uniquely determined by the stimulus waveform $s(t)$ measured in the acoustic coupler and the measured spike times t_i . For a given fibre the filters for two different stimulus ensembles are likely to be different. In the experiments discussed here addition of nonlinear filters to the estimation scheme in equation (1) made negligible quantitative improvements to the estimates.

How do we determine the information transmission rate? We measure the random errors in the estimate, as outlined schematically in figure 1. The estimated stimulus waveform is determined by a compromise between the observed spike train and our a priori knowledge of the stimulus ensemble. When the spike train does not specify the stimulus with complete certainty, a priori knowledge introduces systematic errors in the estimation process. We separate random and systematic errors in the estimate by writing the estimate at each frequency as $\tilde{s}_{\text{est}}(\omega) = g(\omega) [s(\omega) + \tilde{n}(\omega)]$. The gain $g(\omega)$ corrects systematic errors, and the effective noise measures the random errors defined as an input noise level. When both the errors in the estimate and the stimulus itself are Gaussian random variables, the information rate is determined by the signal-to-noise

$$\text{SNR}(\omega) = \langle |\tilde{s}(\omega)|^2 \rangle / \langle |\tilde{n}(\omega)|^2 \rangle,$$

of the estimate as a function of frequency (Shannon 1949),

$$R_{\text{info}} = \frac{1}{2} \int \frac{d\omega}{2\pi} \log_2 [1 + \text{SNR}(\omega)]. \quad (4)$$

The stimuli in our experiments are Gaussian by construction; we must check whether the estimate errors are Gaussian. If there are non-Gaussian errors then equation (4) underestimates the real information transmission rate (Bialek *et al.* 1993), but if the errors are nearly Gaussian then our estimate of R_{info} will be close to the true information rate of the spike train.

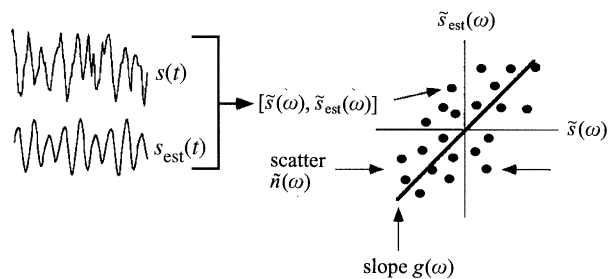


Figure 1. Schematic of calculation of effective noise level. For each experiment we separate random and systematic errors in the estimate by determining a gain $g(\omega)$, which corrects systematic errors, and an effective noise $\tilde{n}(\omega)$ which measures the random errors defined as an input noise level. To determine g and n the stimulus and estimate are divided into 0.25 s segments. We perform a Fourier transform on each segment to obtain a set of points $[\tilde{s}(\omega), \tilde{s}_{\text{est}}(\omega)]$. For each frequency we plot one point from each segment and determine the best fit line through the data; the slope of the line is g and the scatter of the points about the line is n .

3. RESULTS

We characterize the coding in primary afferent fibres by decoding the spike train to estimate the sensory stimulus. The basic strategy of stimulus

estimation or decoding experiments is to learn the rules of the neural code during a fraction of the experiment (80–90% here), and then test our understanding of these rules in a later section of the experiment. The experimental data are the stimulus and spike train; from these we construct the filter F which provides the best estimate of the stimulus from the spikes, as described in the methods. The ‘best estimate’ can be compared directly with the true stimulus. The estimate of the stimulus cannot contain any more information about the true stimulus than the spike train itself, so by analysing the quality of the estimates we put a lower bound on the performance of the neuron as an information transmitting device.

Figure 2 shows amplitude spectra, estimation filters and short sections of the spike train, stimulus waveform and estimate for broad-band and call-spectrum stimuli. An obvious difference between the two experiments is the temporal width of the filters; a spike in the broad-band noise experiment contributes to the estimate for a period of 5–10 ms, while a spike in the call-spectrum experiment contributes for 100–200 ms. The width of the filter in the broad-band experiment is set by the tuning characteristics of the fibre. The fibre’s sensitivity to a limited range of frequencies introduces a correlation time to the signal coded by the spikes, and a

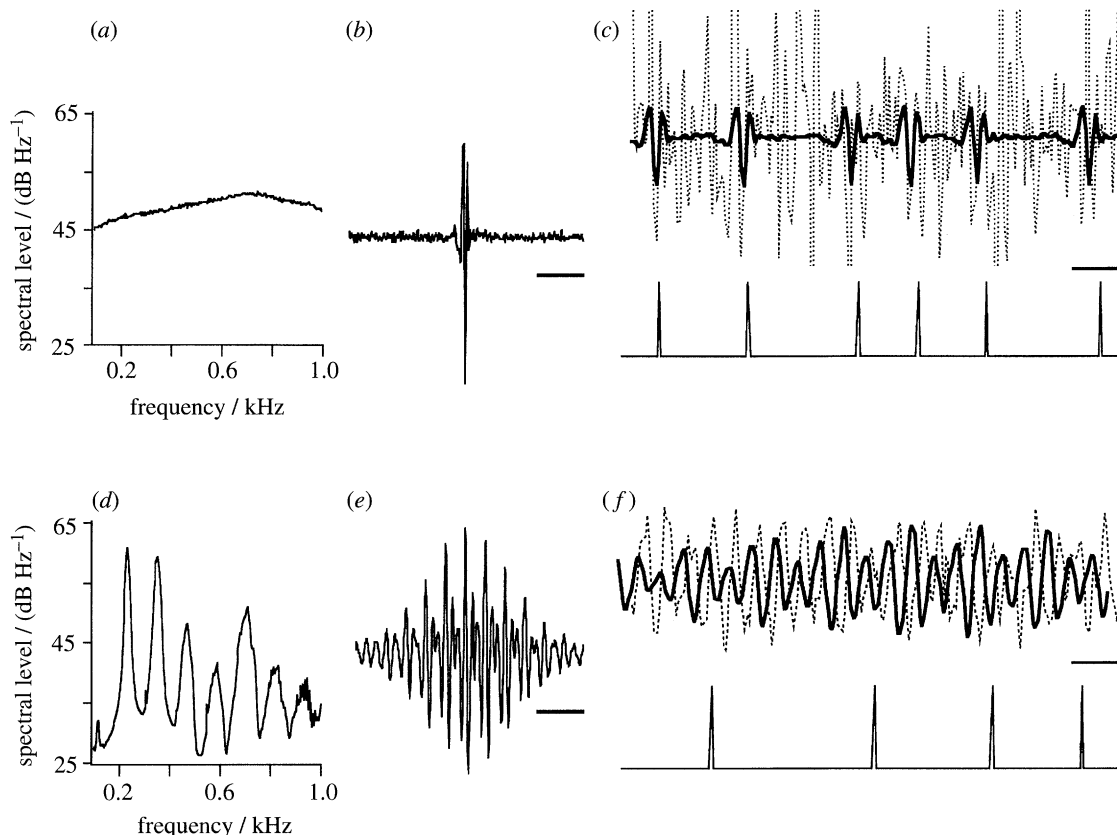


Figure 2. Construction of stimulus estimates. Power spectra of the sound pressure waveform for the broad-band noise (a) and call-spectrum stimuli (d). To study the relation between the stimulus waveform and the spike response, we estimate the stimulus waveform from the spikes by filtering the spike train, as described in the text and Bialek *et al.* (1991). Estimate filters are calculated from the first 90% of the data and tested on the last 10%; the filters for this experiment are shown in (b) (broad-band noise) and (e) (call-spectrum). Convolution of these filters with the spike train produces our estimate of the stimulus waveform. Short sections of the measured spike train, stimulus, and estimated stimulus are shown in (c) (broad-band noise) and (f) (call-spectrum). Timing bars in (b) and (e) are 20 ms; in (c) and (f) the bars are 10 ms.

Table 1. *Collected results from ten low-frequency fibres*

(The BEF for each fibre is determined from measurements of firing rate versus frequency of a pure tone. The information rates and coding efficiencies are measured for a timing precision of $\Delta\tau = 1$ ms, and are quoted with standard deviations calculated by calculating each quantity in each of four sections of the experiment. Although the information rates and efficiencies vary broadly among the cells, the efficiency of the call-spectrum stimulus is consistently much higher than the broad-band stimulus.)

BEF (Hz)	firing rate (spikes per second)		information rate (bits per second)		coding efficiency	
	BBS ^a	CSS ^b	BBS	CSS	BBS	CSS
200	62	65	24 ± 1	130 ± 5	0.073 ± 0.003	0.37 ± 0.02
240	58	46	54 ± 3	181 ± 7	0.17 ± 0.01	0.65 ± 0.03
240	20	32	9 ± 1	35 ± 1	0.064 ± 0.006	0.17 ± 0.01
245	10	23	17 ± 1	89 ± 3	0.18 ± 0.01	0.71 ± 0.03
310	53	77	37 ± 2	268 ± 7	0.13 ± 0.01	0.69 ± 0.02
330	34	17	23 ± 1	111 ± 4	0.11 ± 0.01	0.89 ± 0.03
380	27	28	13 ± 1	82 ± 3	0.12 ± 0.01	0.45 ± 0.02
390	49	32	13 ± 1	71 ± 3	0.064 ± 0.004	0.34 ± 0.02
510	42	50	30 ± 1	131 ± 4	0.12 ± 0.01	0.46 ± 0.02
550	33	26	9 ± 1	68 ± 3	0.047 ± 0.002	0.35 ± 0.02

^a Broad-band stimulus data.

^b Call-spectrum stimulus data.

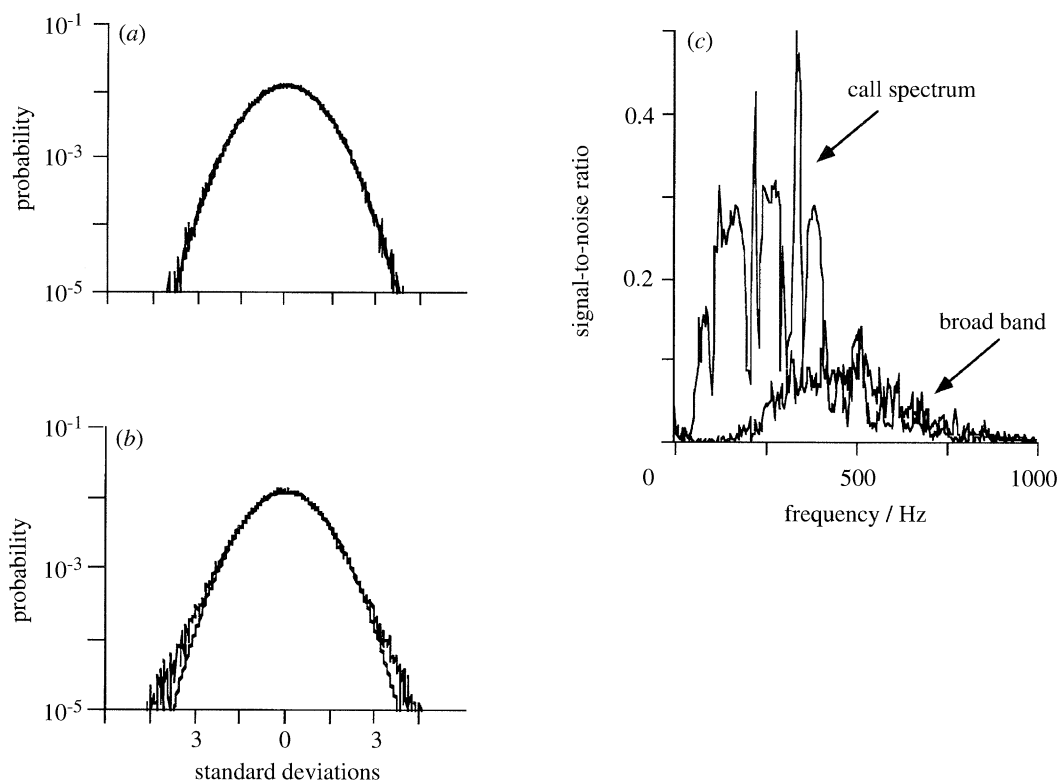


Figure 3. Quantitative characterization of the estimates. (a) Distribution of effective noise amplitudes. The effective noise at each frequency is normalized by its standard deviation. The normalized noise amplitudes are used to create the histogram shown. A Gaussian of unit standard deviation is plotted with each histogram for comparison; the random errors in both experiments are well described by a Gaussian distribution. (b) Signal-to-noise ratio of the estimates. Both the stimulus and noise are Gaussian random variables, so the signal-to-noise ratios are obtained by dividing the stimulus power spectrum, $S(\omega) = \langle |\hat{s}(\omega)|^2 \rangle$, by the effective noise power, $N(\omega) = \langle |\hat{n}(\omega)|^2 \rangle$. The signal-to-noise of the shaped spectrum is significantly higher than the SNR of the broad-band noise over a wide range of frequencies.

single discrete spike contributes to the estimate for a finite time period. In the call-spectrum experiment the correlation time of the stimulus itself is longer than the correlation time introduced by the fibre's tuning; as a result, a single spike contributes to the estimate for a

longer time period. Does the introduction of this correlation time increase the effectiveness of the coding process? Qualitatively comparing the estimates in figure 2 the answer seems to be yes.

We quantify the results of figure 2 by calculating the

rate at which each estimate provides information about the stimulus. The information rate (measured in bits per second) indicates how much a spike train reduces our uncertainty about the stimulus waveform. Before observing the spikes, our uncertainty in estimating the stimulus is large because we know only that the stimulus came from a particular set or ensemble: the ensemble of stimuli with a particular amplitude spectrum. Observation of the spike train reduces our uncertainty in the stimulus, or equivalently reduces the number of possible stimulus waveforms. The information rate measures the difference in the variance or entropy of the distribution of possible stimuli before and after observation of the spike train.

We define an effective noise which measures the random errors in the estimate (see figure 1); this noise determines how accurately an observer of the spike train in a single afferent can estimate the sensory stimulus. The distribution of effective noise amplitudes is nearly Gaussian for both the broad-band and the call-spectrum stimuli (see figure 3*a*). Thus, as discussed in the methods, we can define a meaningful effective noise measure at each frequency and accurately measure the information rate from the signal-to-noise ratio (SNR). SNRs for the fibre in figure 2 are shown in figure 3*c*. The SNR of the call-spectrum stimulus is significantly higher than the SNR of the broad-band stimulus at most frequencies. This increase in SNR occurs even at frequencies where the power in the call-spectrum stimulus is 10–15 dB below that of the broad-band noise; furthermore, the increase in SNR occurs in experiments in which the spectral amplitude at the peaks in the call-spectrum stimulus is equal to the spectral amplitude of the broad-band stimulus. These results indicate that the SNR at one frequency depends on the amplitude of other frequency components of the stimulus—i.e. the system is not behaving linearly. The SNRs correspond to information rates of 46 ± 1 bits per second (1.4 bits per spike) for the broad-band stimulus and 133 ± 5 bits per second (7.8 bits per spike) for the call-spectrum stimulus. Similar results were obtained in ten cells (see table 1).

The result that sensory neurons transmit more information about structured stimuli was a surprise. Gaussian white noise has the maximum possible entropy per unit time given the total power, so that shaping the stimulus into bands lowers the stimulus entropy and hence the available information. We find, however, that the transmitted information increases. The increase in SNR at frequencies where the signal power has decreased (see figure 3) indicates that the increased information transmission rate is caused by nonlinear coding mechanisms which are matched to the characteristics of the call-spectrum stimulus.

The dramatic improvements in information rate we find for a seemingly small step toward naturalistic stimuli leads us to ask how much additional increase in information rate is possible. We put our measured information rates on an absolute scale by determining an upper bound to the information transfer rates (MacKay & McCulloch 1952; Rieke *et al.* 1993). An optimal coding scheme associates each possible output with a separate input signal; for a neuron, this means

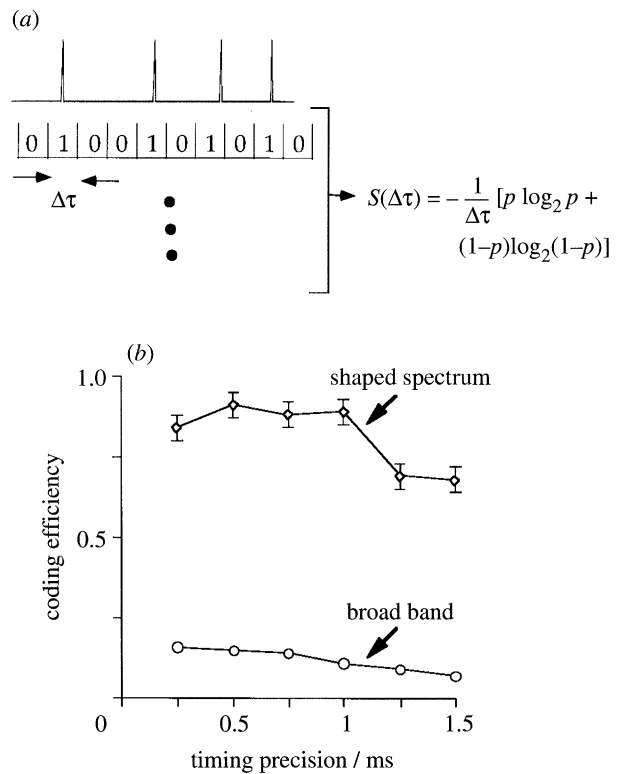


Figure 4. Spike train entropy and coding efficiency. (a) The spike timing precision $\Delta\tau$ and mean firing rate r determine a simple upper bound to the spike train entropy. We digitize the spike train with time bins of width $\Delta\tau$, each of which has a probability $p = r\Delta\tau$ of having a spike and $1-p$ of no spike. Each time bin makes an independent contribution to the entropy. Correlations in the spike trains which cause individual bins not to be independent, such as refractoriness, will cause our simple upper bound to exceed the true entropy. (b) The information rate $R_{\text{info}}(\Delta\tau)$ and entropy rate $S(\Delta\tau)$ determine the coding efficiency, $\epsilon(\Delta\tau) = R_{\text{info}}(\Delta\tau)/S(\Delta\tau)$. Here we plot efficiencies for the call-spectrum stimulus and for broad-band noise. Error bars for the broad-band stimulus are obscured by the data points. Most of the increase in efficiency with the call-spectrum stimulus is due to a higher information rate (133 bits per second versus 46 bits per second for the broad-band stimulus).

each possible spike train represents a different stimulus waveform. The spike train entropy measures the number of degrees of freedom, roughly the number of possible spike trains, given the firing statistics (see figure 4*a*). Since the cell can code only as many stimulus variables as there are degrees of freedom in the spike train, the entropy sets a fundamental upper limit to the information rate. We define the coding efficiency as the ratio of the information rate to the spike train entropy.

If the spike times are specified with infinite precision, the entropy is infinite. Infinite timing precision is impossible, so we introduce a finite timing precision $\Delta\tau$. Because we do not know what the appropriate timing precision is, we calculate the coding efficiency as a function of $\Delta\tau$. We calculate an upper bound to the entropy from the timing precision and the mean interval between spikes for a particular experiment (MacKay & McCulloch 1952; see also figure 4*a*). To determine the information rate as a function of the

spike timing precision, we specify the spike times to a precision $\Delta\tau$ and estimate the stimulus from the re-digitized spike train as described above. We now have the two components of the coding efficiency: the information rate and the entropy rate, both functions of the timing precision for individual spikes. Figure 4*b* shows the coding efficiencies for the cell from figure 2 for the broad-band and call-spectrum stimuli.

Data from ten amphibian papilla fibres ranging in BEF from 200 Hz to 550 Hz are summarized in the table. We focused on fibres in this frequency range because the low-frequency fibres of the amphibian papilla use coding mechanisms similar to those of auditory fibres in other vertebrates. A more limited collection of experiments on higher-frequency fibres from the amphibian papilla showed similar improvements in information rate and coding efficiency. For all the cells studied, the information rate and coding efficiency are significantly higher for the call-spectrum stimulus. The information rate increases by a factor of 5.4 on average, and the coding efficiency a factor of 4.3. The coding efficiency in some cases reaches 90%, indicating that the coding of the call-spectrum stimulus in these afferents comes very close to fundamental limits to information transfer.

4. DISCUSSION

Our initial aim was to determine whether primary auditory afferents are 'tuned' to code natural stimuli with high efficiency. By creating stimuli with a naturalistic amplitude spectrum (but unstructured phase spectrum) we discovered two important characteristics of peripheral coding: (i) stimuli with naturalistic amplitude spectra are coded at higher information rates and efficiencies than broad-band stimuli; and (ii) the coding efficiency of stimuli with naturalistic amplitude spectra can be as high as 90%, approaching the fundamental limit to information transfer. These results indicate that primary auditory afferents are indeed tuned to statistical properties of natural stimuli, and that the amplitude spectrum is of central importance in determining the coding strategy.

In addition to structured amplitude spectra, natural sounds have structured phase spectra. Furthermore, the responses of auditory afferents in the bullfrog are sensitive to the relative phase angle of the frequency components in a stimulus (Simmons *et al.* 1993; Bodnar & Capranica 1994). Thus we were surprised to find that the efficiency coding of stimuli with random phase spectra was close to 100%. Although the phase spectra of our stimulus ensembles are random, the estimation filters do have phase structure which allows estimation of the temporal structure in a particular stimulus waveform from the ensemble. The sensitivity of auditory fibres to relative phase indicates that phase structure in the ensemble of stimuli may also influence coding. For example, a structured phase spectrum may improve the efficiencies in afferents which code random phase stimuli at relatively low efficiencies. The next generation of experiments should quantify these phase effects in information-theoretic terms.

Our results indicate that the dynamics of the coding process in primary auditory afferents are matched to the correlation structure of natural sounds; as a result the system codes natural sounds at higher information rates and efficiencies than white noise. We propose that this improvement in coding occurs because the temporal correlation time of natural stimuli is similar to the time scales for spike generation, such as the mean interval between spikes. This improvement would not be possible if the auditory system acted linearly with additive stimulus-independent noise; if this were the case, lowering the power at a given frequency would lower the SNR at that frequency and broad-band stimuli would provide the highest possible rate of information transfer. Instead nonlinearities in auditory processing increase the information rate and coding efficiency for naturalistic stimuli.

We thank R. R. Capranica for support and encouragement. We also thank D. Ruderman, A. Schweitzer, D. Warland and J. Vrieslander for helpful discussions and A. H. Bass, E. C. Ihle, and D. Warland for comments on the manuscript. Work at Cornell was supported in part by the NEC Research Institute and by the NIH through grant HAR CD-00092 to R. R. Capranica and A. H. Bass.

REFERENCES

- Barlow, H. B. 1961 Possible principle underlying the transformation of sensory messages. In *Sensory communication* (ed. W. Rosenblith), pp. 217–234. Cambridge: MIT Press.
- Bialek, W., Rieke, F., de Ruyter van Steveninck, R. R. & Warland, D. 1991 Reading a neural code. *Science, Wash.* **252**, 1854–1857.
- Bialek, W., DeWeese, M., Rieke, F. & Warland, D. 1993 Bits and brains: information flow in the nervous system. *Physica, A* **200**, 581–593.
- Bodnar, D. A. & Capranica, R. R. 1994 Encoding of phase spectra by the peripheral auditory system of the bullfrog. *J. comp. Physiol.* **174**, 157–171.
- Bogert, C. M. 1960 The influence of sound on the behavior of amphibians and reptiles. In *Animal sounds and communication* (ed. W. E. Lanyon & W. N. Tavolga), pp. 137–320. Washington: American Institute of Biological Sciences.
- Capranica, R. R. 1965 *The evoked vocal response of the bullfrog*. Cambridge: MIT Press.
- Capranica, R. R. 1968 The vocal repertoire of the bullfrog (*Rana catesbeiana*). *Behaviour* **31**, 302–325.
- Capranica, R. R. 1976 Morphology and physiology of of the auditory system. In *Frog neurobiology* (ed. R. Llinás & W. Precht). Berlin: Springer-Verlag.
- Capranica, R. R. & Moffat, A. J. M. 1975 Selectivity of the peripheral auditory system of spadefoot toads (*Scaphiopus couchii*) for sounds of biological significance. *J. comp. Physiol.* **100**, 231–249.
- Capranica, R. R. & Moffat, A. J. M. 1980 Nonlinear properties of the peripheral auditory system of anurans. In *Comparative studies of hearing in vertebrates* (ed. A. N. Popper & R. Fay), pp. 139–165. New York: Springer.
- Freedman, E. G., Ferragamo, M. & Simmons, A. M. 1988 Masking patterns in the bullfrog (*Rana catesbeiana*). II: Physiological effects. *J. Acoust. Soc. Am.* **84**, 2081–2091.
- Frishkopf, L. S., Capranica, R. R. & Goldstein, M. H. 1968 Neural coding in the frog's auditory system: a teleological approach. *Proc. I.E.E.E.* **56**, 969–980.

- Liff, H. & Goldstein, M. H. 1970 Peripheral inhibition in auditory nerve fibers in the frog. *J. Acoust. Soc. Am.* **47**, 1538–1547.
- MacKay, D. & McCulloch, W. 1952 The limiting information capacity of a neuronal link. *Bull. Math. Biophys.* **14**, 127.
- Narins, P. M. & Hillery, C. M. 1983 Frequency coding in the inner ear of anuran amphibians. In *Hearing – physiological basis and psychophysics* (ed. R. Klinke & R. Hartmann), pp. 70–76. Berlin: Springer-Verlag.
- Rieke, F., Yamada, W., Moortgat, K., Lewis, E. R. & Bialek, W. 1991 Real-time coding of complex sounds in the auditory nerve. In *Auditory physiology and perception: proceedings of the 1991 European hearing workshop* (ed. Y. Cazals, L. Demany & K. Horner), pp. 315–321. Oxford: Pergamon.
- Rieke, F., Warland, D. & Bialek, W. 1993 Coding efficiency and information rates in sensory neurons. *Europhys. Lett.* **22**, 151–156.
- Ruderman, D. L. & Bialek, W. 1994 Statistics of natural images: scaling in the woods. *Phys. Rev. Lett.* **73**, 814–817.
- Shannon, C. E. 1949 Communication in the presence of noise. *Proc. I.R.E.* **37**, 10–21.
- Shannon, C. E. & Weaver, W. 1964 *The mathematical theory of communication*. Urbana: University of Illinois Press.
- Shofner, W. P. & Feng, A. S. 1981 Post-metamorphic development of the frequency selectivities and sensitivities of the peripheral auditory system of the bullfrog, *Rana catesbeiana*. *J. exp. Biol.* **93**, 181–196.
- Shraiman, B. I. & Siggia, E. D. 1994 Lagrangian path integrals and fluctuations in random flow. *Phys. Rev. E.* **49**, 2912–2927.
- Simmons, A. M., Reese, G. & Ferragamo, M. 1993 Periodicity extraction in the anuran auditory nerve II: phase and temporal fine structure. *J. Acoust. Soc. Am.* **93**, 3374–3389.
- Warland, D., Landolfi, M. A., Miller, J. P. & Bialek, W. 1991 Reading between the spike in the cercal filiform hair receptors of the cricket. In *Analysis and modeling of neural systems* (ed. F. Eeckman), pp. 327–333. Norwell: Kluwer.

Received 9 June 1995; accepted 25 June 1995